

NUMERICAL SIMULATION OF JET IMPINGEMENT COOLING ON A PIN-FIN

Keshab Jagat

NUMERICAL SIMULATION OF JET IMPINGEMENT COOLING ON A PIN-FIN

*Thesis submitted to the
National Institute of Technology, Rourkela
for the award of the degree
of*

Master's of Technology in cryogenic and Vacuum Technology

by

Keshab Jagat

Under the guidance of

Dr. Amitesh Kumar



**DEPARTMENT OF MECHANICAL ENGINEERING
NATIONAL INSTITUTE OF TECHNOLOGY, ROURKELA**

JUNE 2015

©2015 keshab Jagat. All rights reserved.

CERTIFICATE

This is to certify that the thesis entitled **Numerical Simulation of Jet Impingement Cooling on Pin-Fin**, submitted by **Keshab Jagat** to National Institute of Technology, Rourkela, is an authentic record of bona fide research work carried under my supervision and I consider it worthy of consideration for the award of the degree of Master's of Technology of the Institute.

Date :

Dr. Amitesh Kumar

Assistant Professor

Department of Mechanical Engineering

National Institute of Technology

Rourkela, 769008

DECLARATION

I certify that

1. The work contained in the thesis is original and has been done by myself under the general supervision of my supervisor.
2. The work has not been submitted to any other Institute for any degree or diploma.
3. I have followed the guidelines provided by the Institute in writing the thesis.
4. Whenever I have used materials (data, theoretical analysis, and text) from other sources, I have given due credit to them by citing them in the text of the thesis and giving their details in the references.

Keshab Jagat

CURRICULUM VITA

Name: Keshab Jagat

Educational Qualification:

<u>Year</u>	<u>Degree</u>	<u>Subject</u>	<u>University</u>
2013	B.E	Mechanical engineering	Biju Patnaik University of Technology, Rourkela

ACKNOWLEDGEMENTS

I want to give special thanks to my supervisor Dr. Amitesh Kumar for offering me his extensive knowledge in Jet impingement cooling and his patience, guidance, helps and encouragements to me. His academic manner and his approach to problems will benefit me in my future study and life. I thank him for supporting my study in NIT, Rourkela. I also want to give my appreciation to my lab-mates Prasad Parag Wadile and Vishnu Rajpuria, for their supports and valuable suggestions for my research. During my Simulation, my friends Manoj Kumar and Laxman Chawhan gave me lots of helps and valuable suggestions. Specially thanks to Tej pratap singh who is there for me in every path. Without them, I cannot finish my researches so quickly and smoothly. I would thank them for all they did for me.

Date :

Keshab Jagat

Place :

Contents

Certificate	
Declaration	i
Curriculum Vita	ii
Acknowledgements	iii
Contents	iv
List of Figures	vi
List of Tables	viii
List of Symbols and Abbreviations	ix
Abstract	i
1 Introduction	1
1.1 Review of Literature	2
1.2 Definition of the problem	4
1.3 Objectives and methodology	4
2 Numerical simulation	6
2.1 Governing differential equation	7
2.1.1 Assumptions	7
2.1.2 Boundary conditions	9

2.2 Numerical modelling	10
2.2.1 Method of solution	10
2.2.2 Solution Approach	11
3 Results and Discussions	12
3.1 Heat transfer and fluid flow characteristics of axis symmetry enclosure with Reynolds number 3078	13
3.1.1 Flow Characteristics	14
3.1.2 Heat transfer characteristic	17
3.2 Heat transfer and fluid flow characteristics of axis symmetry enclosure with Reynolds number 5019	20
3.2.1 Flow Characteristics	20
3.2.2 Heat transfer characteristic	24
3.3 Heat transfer and fluid flow characteristics of axis symmetry enclosure with Reynolds number 8673	27
3.3.1 Flow Characteristics	27
3.3.2 Heat transfer characteristic	30
3.4 Tabular form of results	33
4 Conclusion and future work	35
4.1 CONCLUSION	35
4.2 Future works	36
Bibliography	37

List of Figures

2.1	Computational Domain	8
2.2	maished domain	8
2.3	Domain representing boundary type	9
3.1	vector plots for $\frac{C}{r} - 2.23, Re - 3078$	14
3.2	Vector plot for $\frac{C}{r} - 5.5, Re - 3078$	15
3.3	Vector plot for $\frac{C}{r} - 8.77, Re - 3078$	16
3.4	isothermal plot for $\frac{C}{r} - 2.23, Re - 3078$	17
3.5	isothermal plot for $\frac{C}{r} - 5.5, Re - 3078$	18
3.6	isothermal plot for $\frac{C}{r} - 8.77, Re - 3078$	19
3.7	vector plots for $\frac{C}{r} - 2.23, Re - 5019$	21
3.8	Vector plot for $\frac{C}{r} - 5.5, Re - 5019$	22
3.9	Vector plot for $\frac{C}{r} - 8.77, Re - 5019$	23
3.10	isothermal plot for $\frac{C}{r} - 2.23, Re - 5019$	24
3.11	isothermal plot for $\frac{C}{r} - 5.5, Re - 5019$	25
3.12	isothermal plot for $\frac{C}{r} - 8.77, Re - 5019$	26
3.13	vector plots for $\frac{C}{r} - 2.23, Re - 8763$	27
3.14	Vector plot for $\frac{C}{r} - 5.5, Re - 8763$	28
3.15	Vector plot for $\frac{C}{r} - 8.77, Re - 8763$	29

3.16 isothermal plot for $\frac{C}{r} - 2.23$, $Re - 8763$	30
3.17 isothermal plot for $\frac{C}{r} - 5.5$, $Re - 8763$	31
3.18 isothermal plot for $\frac{C}{r} - 8.77$, $Re - 8763$	32
3.19 Jet-to-nozzle spacing v/s Nusselt number	34

List of Tables

2.1	Boundary condition	9
3.1	Parameter table	13
3.2	Average Nusselt number for different $\frac{C}{r}$ ratio	33

LIST OF SYMBOLS AND ABBREVIATIONS

Nu	Local Nusselt Number
H_f	Height of Fin
W	Width of the Fin
C	Jet-to-Fin spacing
\overline{Nu}	Average Nusselt number
Re	Reynolds Number
r	Width of the nozzle
C/r	Ratio between the jet-to-fin spacing and nozzle width
H_f/r	Ratio between the height of fin and nozzle width
W/r	Ratio between the width of fin and nozzle width
T_w	Temperture along the surface
T_f	Bulk Temperature
C	jet-to fin spacing
w	width of fin
H_f	length of fin
l	characterstic length
h	convective heat transfer
q''	Heat flux

Greek symbols

μ	Viscosity of fluid
ν	Kinematic viscosity of fluid
ρ	Density of fluid

Abstract

The study of a laminar natural convection in a domain with conjugate boundary condition is done by numerical simulation. The Bottom wall of the enclosure is considered to be isothermal. The problem is solved using Ansys Package 15 and the fluent is used for meshing the domain. Various cases are considered by varying the parameters like Reynolds number, jet-to-fin spacing, width of fin and Height of Fin to analyse their effect on the heat transfer and flow characteristics. Reynolds number is taken equal to 3078, 5019 and 8673 to constrain the flow as laminar in enclosure. The result shows some significant dependence on Reynolds number and jet-to-fin spacing in the flow and temperature field inside the domain.

Keywords: jet impingement cooling, heat transfer in fin, laminar, natural convection

CHAPTER 1

Introduction

The fluid stream flow from a jet/nozzle with a high velocity and high kinetic energy term as Jet. The fluid at high velocity impinges on the vane or a plate through a fluid jet is known as Jet impingement. Due to the ability of achieving high heat transfer rates the impinging jet is an effective cooling mechanism. Due to its ability of high heat transfer it is widely used in the industry for various applications such as annealing of metals, gas turbine blades cooling, photovoltaic cells cooling and heat cooling during grinding processes. Jet impingement also used for direct electronic cooling for high-powered electronic components and photonic thermal management solutions. Nozzle geometry and also have a significant influence on heat transfer.

Numbers of articles could be found in the literature review for studying the jet impingement cooling on fin. . Most of the already studied jet impingement cooling are either cooling on flat plate, cooling of pin-fin using multi-jet nozzle and cooling of electronic component. But in present study we have considered the boundary condition which are practically applicable with conjugate heat transfer.

1.1 Review of Literature

In past two decade, jet impingement heat transfer has received considerable attention due to its application for high heat transfer rates. There are many researchers deals with both experimental and numerical study. The most recent review which deal with jet impingement cooling are described by Webb & Ma (1995), Viskanta (1993) and Jambunathan et al. (1992)[10]. The heat transfer rate in a jet impingement are affected by number of parameters. such as jet-to-plate spacing not only affects the rate of heat transfer but it also affects the local heat transfer coefficient distribution. The importance of the parameters should be characterized for the designing and analysis of jet impingement heating or cooling system[15]. In some of the review the effect of parameters has been studied and results obtained from the experiments by different researchers have been explained. Jambunathan et al. in his study clearly find out the problem and explained that, for better understanding of the jet impingement cooling, the detail of the geometry and flow are required, so that different experimental data can be compared[10]. Garimella and Rice and Fitzgerald and Garimella[8][6] studied and noted that the confinement of the jet impingement results in one or more recirculating toroidal patterns formation as the discharges of flow along the target zone. Obot et al. Studied and observed that if local heat transfer coefficients is reduced on the order of 50% as a result of confining the air outflow. The effect of confinement is evident up to jet-to-target plate spacings of four to five nozzle diameters. San et al. showed that the confined jet impingement having recirculating flow at high Reynolds numbers brings heated air back into the jet, thus in the stagnation region degrading heat transfer formed[14]. This heat transfer reduction was confirmed for liquid jets by Garimella and Rice[8]. Zuckerman and Lior and Weigand and spring numerically and experimentally studied the correlative parameters of jet impingement, which include pattern of jet array, inlet Reynolds number, jet-to-jet spacing, jet-to-plate spacing[17][16].

The jet impingement research over a smooth target plate was very sufficient. According to Florschuetz[7] the inline jet array and staggered arrays, compare to staggered array performance of inlinejet is better in the terms of average heat transfer rates. According

to Weigand and Spring[16] review on characteristics of heat transfer on multi impinging jet, opposing heat transfer surface area was considered to be 1-4%, which is equivalent to the jet-to-jet spacing with jet diameter having 4-6. Where the optimum ratio between jet to jet spacing and jet diameter is considered between 1 and 3. The relation between the jet to plate spacing to the jet core lengths on the heat transfer performance was observed by Golstein in array of jet impingement[9]. Florschuetz[7] studied the crossflow effect and found that due to sweep away of jet and delay impingement it may affect the heat transfer performance in many cases. Chambers et al.[3] observed that from the small inlet crossflow large quantity of heat can be transferred.

The Jet impingement used as a cooling technique and due to its thin temperature and velocity boundary layer which is formed due to its speed impingement it is more efficient. The factor which is responsible for the heat transfer is physical parameters, operating parameters and structural parameters. Recently Garimella and Lie[11] developed a correlation between Nusselt number and stagnation point, using some correlation for Prandtl number, Reynolds number, jet diameters and standoff ratio. Sun et al.[14] also develop a correlation between Nusselt number and stagnation point and the correlation was compared using three different fluids against his experimental data. The fluid which is used is R113, Kerosene and transformer oil with inlet diameter 0.987mm and 35 mm length with constant heat flux.

During the period 1999 to 2001 many researchers[6] were interested in jet impingement, Garimella and Brignoni and EL-Sheikh and Garimella done various research and published article on heat transfer and optimization of single and multiple jet on pin fin using air as cool their coolant[2][5]. They also studied using various jet diameters, Reynolds number. Ekkad and Kontrovitz[4] using the work related to Sullivan et al.(2002) studied the effect of heat transfer distribution over a dimples using jet impingement using transient liquid crystal techniques, using Reynolds numbers(4800-14800) heat transfer rate was calculated. On the same year Maveety and Jung numerically and experimentally investigate and obtained the result for heat transfer from square pin-fin heat sinks which is subjected to air jet impingement. Here five square pin-fin were investigated using

different Reynolds number varied from 9690 to 26,050. And all other parameter such as heat sinks, fin height, base thickness and jet diameter as 15mm, 5.03mm, 6.4mm respectively. And its show lower thermal resistance over the Reynolds number and significant thermal resistance for other parameters[13]. Li et al. studied the effect of the impinging Reynold number, distance between the tip of the fin and nozzle on the thermal resistance, width and height of the fin[12]. Thermal performance of plate-pin fin heat sink and plate fin heat sink was numerically studied by Yu. Peles et al. investigate the pressure drop and heat transfer over a micro pin-fin fin. Yang in his studied described about the effect of heat transfer coefficient of pin-fin heat sink with different cross-section and arrangement.

1.2 Definition of the problem

When we discuss about the jet impingement cooling it covers a wide area of interest, from industry to medical where heat is to be removed. The present study was motivated from the researcher who are already study the effect of local heat transfer coefficient using jet impingement in laminar flow. Very few are taken interested to study the laminar flow in pin-fin. The effect of different parameter with different Reynolds number, are studied in the present work. The comparison of the result give us the idea about the parametric range to be considered during cooling or heat removing from any hot surface.

1.3 Objectives and methodology

The main objective behind the simulation was to study the effect heat transfer and flow characteristics of the air which is used during the simulation for various parameters. The model is developed using Ansys 15 for this problem and non-dimensionalised study was carried out so that the model could be applied for various scale. The results which are obtained from the present study will also give a reference for further developing of Ansys model and experimental model for jet impingement cooling for conjugate heat transfer.

to obtain the objective of the study we go through following stage:-

- **Stage 1. Literature survey :-** study of already discussed problem for jet impingement cooling was investigated in published article in various SCI journals was done.
- **Stage 2. Ansys Model :-** Using different solution method in Ansys, the results were calculated.
- **Stage 3. Model Assessment :-** A detail parametric study for understanding the effect of boundary condition on the selected domain was done.
- **Stage 4. Result Analysis :-** The result obtained was discussed thoroughly with the help of plot and graph for different parameters.

CHAPTER 2

Numerical simulation

Initially an two dimensional axis symmetry enclosure was considered with given boundary condition which is filled with air. the computational domain and maished domain shown in the figure2.12.2. Then an isothermal condition was provided in the bottom wall and fin to study its effect. All the boundary condition which are shown in the figure having different and practical boundary condition. The vertical/left wall and fin is considered to be isothermal at high temperature and nozzle inlet having constant low temperature. Numbers of cases was studied by varying the jet-to-nozzle spacing, width of fin, length of fin and for each case the Reynolds number are varied to study the effect of the above parameter in flow and temperature field of fluid in enclosure.

2.1 Governing differential equation

The governing equations for two dimensional, steady state flow are presented as continuity equation,

$$\frac{\partial}{\partial x}(\rho u) + \frac{\partial}{\partial y}(\rho v) = 0$$

u-momentum equation,

$$\frac{\partial(\rho uu)}{\partial x} + \frac{\partial(\rho vu)}{\partial y} = \frac{\partial}{\partial x}\left(\mu \frac{\partial u}{\partial x}\right) + \frac{\partial}{\partial y}\left(\mu \frac{\partial u}{\partial y}\right) - \frac{\partial p}{\partial x}$$

v-momentum, equation,

$$\frac{\partial(\rho vu)}{\partial x} + \frac{\partial(\rho vv)}{\partial y} = \frac{\partial}{\partial x}\left(\mu \frac{\partial v}{\partial x}\right) + \frac{\partial}{\partial y}\left(\mu \frac{\partial v}{\partial y}\right) - \frac{\partial p}{\partial y}$$

energy equation,

$$\rho c_p \left(u \frac{\partial T}{\partial x} + v \frac{\partial T}{\partial y} \right) = \frac{\partial}{\partial x} \left(k \frac{\partial T}{\partial x} \right) + \frac{\partial}{\partial y} \left(k \frac{\partial T}{\partial y} \right)$$

2.1.1 Assumptions

The domain is assumed to be two dimensional axis symmetry with laminar natural convection mode of heat transfer. All the properties of the fluid taken in the simulation is considered to be constant.

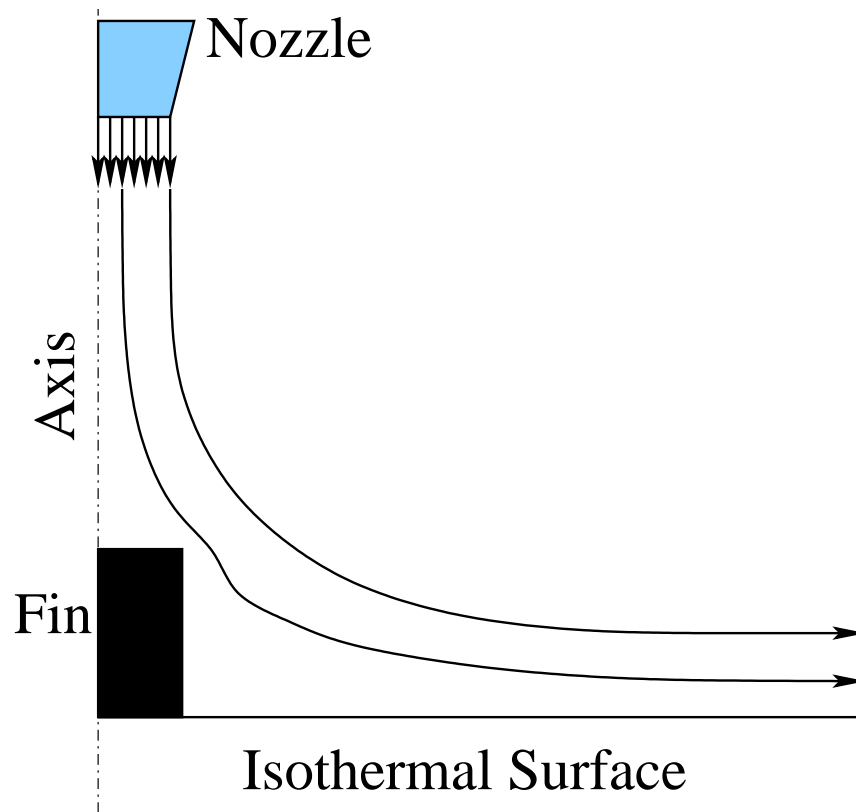


Figure 2.1: Computational Domain

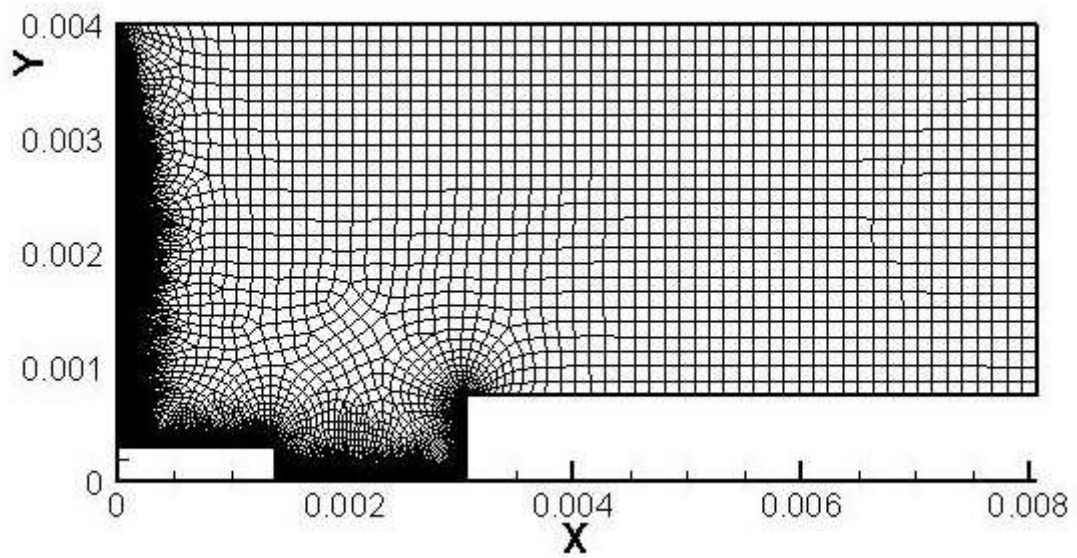


Figure 2.2: maished domain

2.1.2 Boundary conditions

All the five boundary condition of the domain are maintained at different boundary condition as shown in figure 2.3 and table 2.1. The nozzle inlet is maintained at lower temperature i.e. velocity inlet with velocity specification method as component and reference frame as relative to adjacent with constant axial velocity. The top wall and right wall is considered to be pressure outlet with constant pressure and high temperature. The left wall and fin are considered to be isothermal maintained at high temperature in the whole domain with stationary wall and no slip condition. The side wall of the nozzle is considered to be stationary wall with no slip condition with constant high temperature. And the Axis as axis.

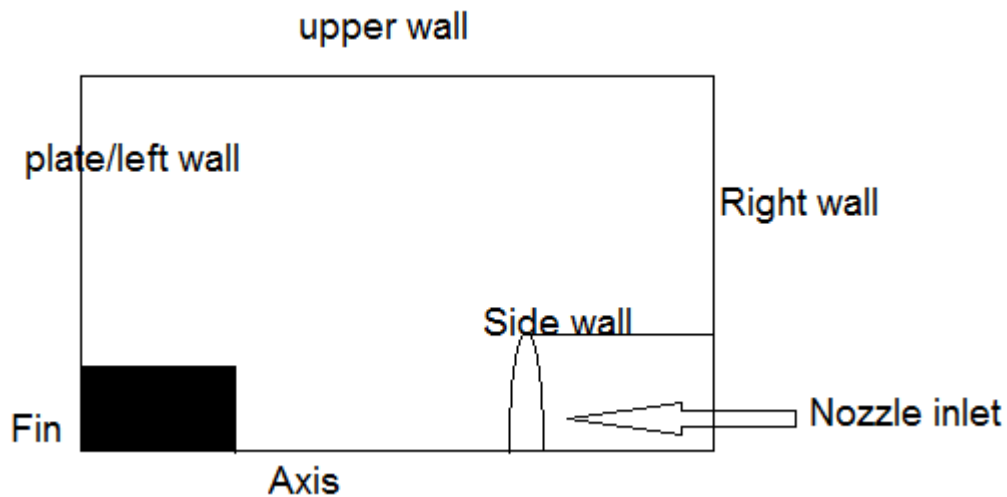


Figure 2.3: Domain representing boundary type

Table 2.1: Boundary condition

Boundary type	Boundary condition
Nozzle/inlet	velocity inlet
side wall	wall
plate/left wall and fin	stationary wall
right wall and top wall	pressure outlet
Axis	axis

2.2 Numerical modelling

The method which is most commonly followed in the past is based on the Patankar's method. This method is based on the assumption of the high viscosity value for the solid region when conjugate heat transfer is to be considered. So, the whole domain can be considered as one and with such assumption the velocity term can be neglected in the solid zone and simultaneous solution of the equation is possible. Thus, the energy equation is solved for fluid region. And few other methods developed in the recent past involves the immersed boundary condition and ghost node method.

2.2.1 Method of solution

The solution method used is pressure-velocity coupling. Pressure- velocity coupling is preprocessed method which is used for study of steady flow problem in CFD. There are four type of scheme under the pressure- velocity coupling such as simple algorithm which stands for Semi- Implicit method for pressure-linked equations. Guess and correct procedure used for the calculation of the staggered grid pressure field. Simplec algorithm is just copy of simple algorithm, except that the manipulations are changed to ensure lesser omissions. Piso is generally used for the turbulent flow. The solution scheme used in the present study is simple. The pressure is taken as second order and momentum and energy are taken as second order upwind.

The governing equations are solved using finite volume approach. The semi-implicit method for pressure linked equation (SIMPLE) is used to couple momentum and continuity equations.

2.2.2 Solution Approach

The formula used to find out the Nusselt number

$$Nu = \frac{hd}{k}$$

h =convective heat transfer,

k =Thermal conductivity of air,

d = characteristic length

The formula which is used for calculation of convective heat transfer

$$h = \frac{q''}{T_w - T_f}$$

To calculate the T_w and T_f point and line are created in the Fin and flat plate of Domain, using ansys fluent where surface is selected to create point and line, then using area weight average and mass weight average for total temperature the point and line temperature was calculated. For heat flux mass weight average with total heat flux was used in fluent to calculate its value.

velocity was calculated using the relation between nusselt number and velocity which give a formula

$$Re = \frac{\rho v d}{\mu}$$

Average nusselt number was calculated using origin pro where distance and local nusselt number data were given, and origin pro give us area under the curve, by dividing the area under the curve with total length the \overline{Nu} was calculated.

CHAPTER 3

Results and Discussions

Two dimensional laminar natural convection of an air filled axis symmetry domain is studied for different parameters such as characteristics of Reynolds number, jet-to-nozzle spacing, width of nozzle and height of nozzle. Reynolds number is varied between 3000 and 9000 as shown in table 3.1 . To study the effect of jet-to-plate spacing on the heat transfer characteristics, and C/r ratio is varied as 2.23, 5.5 and 8.77 . The isothermal contours and velocity vectors are presented. The thermal conductivity of fluid, i.e. air is considered to be 0.0242 W/m-K.

The results show some interesting facts and phenomenon which were unexpected at the early stage of our investigation. Simulations for various parameters were carried with the same domain and effects of various parameters on the result are presented. They are shown in tabular form in the following part and an effort to correlate them are made . Reynolds number is considered so as to have the laminar flow inside the enclosure. Another parameter which could not be neglected for the problem specified here is fin width and height of the fin. thus, the effect of fin width and height of fin is studied and varied with $\frac{H_f}{r}$ ratio and $\frac{w}{r}$ ratio .

$\frac{C}{r}$	$\frac{H_f}{r}$	$\frac{w}{r}$	Re. no.
2.23	1.85	0.4	3078
5.5	2.31	0.54	5019
8.77	2.77	0.68	8673
—	3.08	0.77	—

Table 3.1: Parameter table

3.1 Heat transfer and fluid flow characteristics of axis symmetry enclosure with Reynolds number 3078

A 2-D Axis-symmetry domain is considered with a nozzle and fin over a plate on the left side of the domain. This imposes the conjugate nature of heat transfer. The laminar natural flow is induced inside the domain. In the following section the detail parametric study is carried out discussing the effect of this various parameters.

3.1.1 Flow Characteristics

The velocity vector shown in the figure 3.1, 3.2 and 3.3 are observed to change according to the $\frac{C}{r}$ ratio but its variation with $\frac{H_f}{r}$ and $\frac{W}{r}$ ratio is less. The velocity of fluid is low for the lower jet-to-plate spacing as compare to high jet-to fin spacing as shown in figure 3.1d and 3.3d. Also, it can be observed that for low jet-to-fin spacing bounce back effect can be clearly seen on the corner of vertical/left wall and fin. The upper side and right side area of the domain for higher width and height of fin is seen to be stagnant, which shows very less flow or no flow at all.

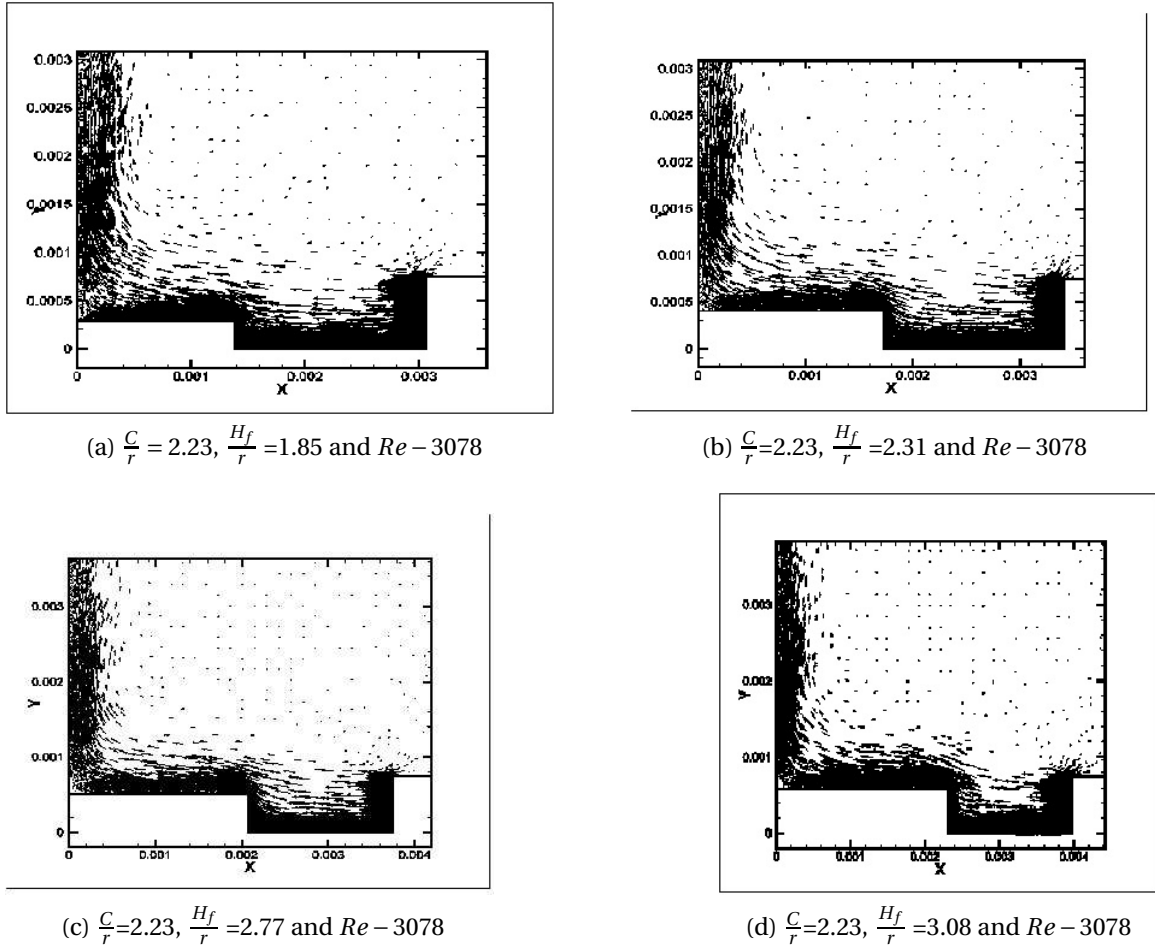
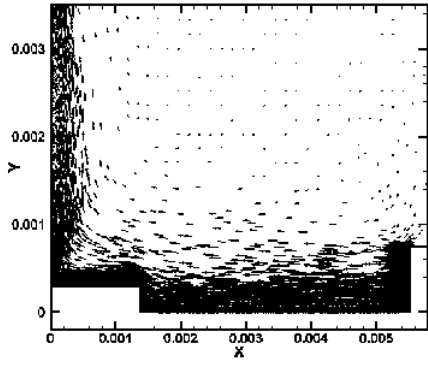
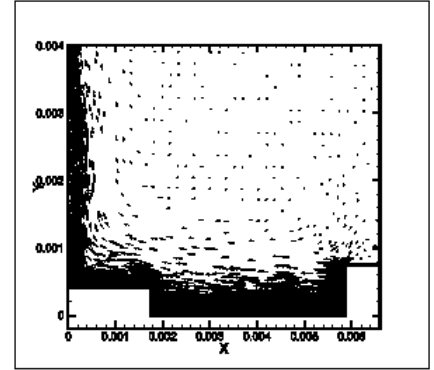


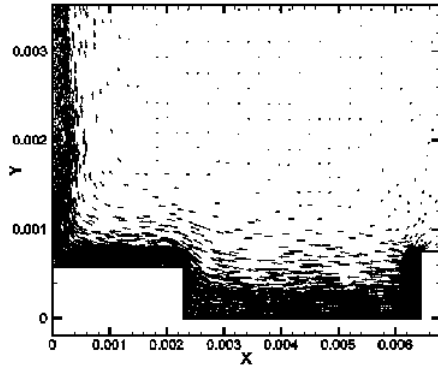
Figure 3.1: vector plots for $\frac{C}{r} = 2.23$ $Re = 3078$



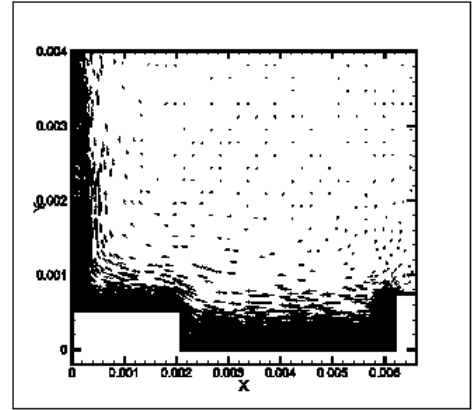
(a) $\frac{C}{r}=5.5$, $\frac{H_f}{r}=1.85$ and $Re=3078$



(b) $\frac{C}{r}=5.5$, $\frac{H_f}{r}=2.31$ and $Re=3078$

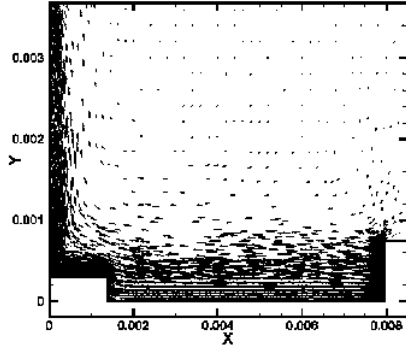


(c) $\frac{C}{r}=5.5$, $\frac{H_f}{r}=2.72$ and $Re=3078$

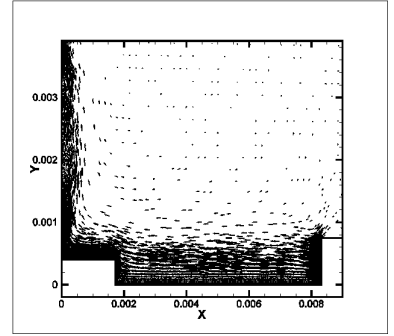


(d) $\frac{C}{r}=5.5$, $\frac{H_f}{r}=3.08$ and $Re=3078$

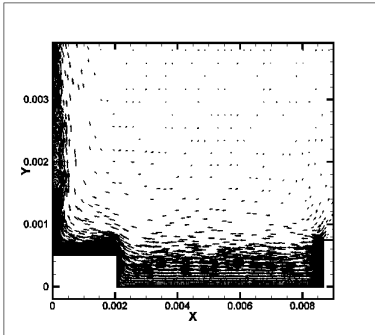
Figure 3.2: Vector plot for $\frac{C}{r}=5.5$, $Re=3078$



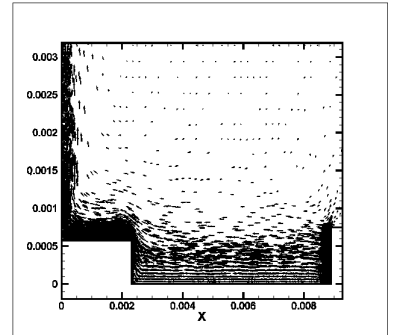
(a) $\frac{C}{r} = 8.77$, $\frac{H_f}{r} = 1.85$ and $Re = 3078$



(b) $\frac{C}{r} = 8.77$, $\frac{H_f}{r} = 2.31$ and $Re = 3078$



(c) $\frac{C}{r} = 8.77$, $\frac{H_f}{r} = 2.77$ and $Re = 3078$

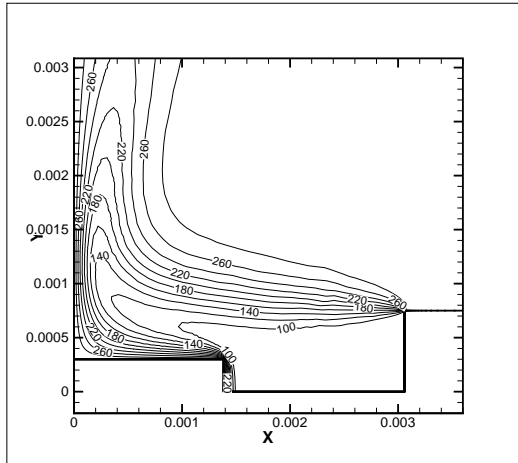


(d) $\frac{C}{r} = 8.77$, $\frac{H_f}{r} = 3.08$ and $Re = 3078$

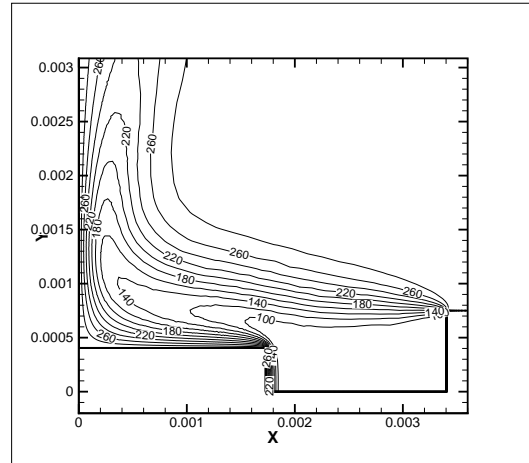
Figure 3.3: Vector plot for $\frac{C}{r} = 8.77$, $Re = 3078$

3.1.2 Heat transfer characteristic

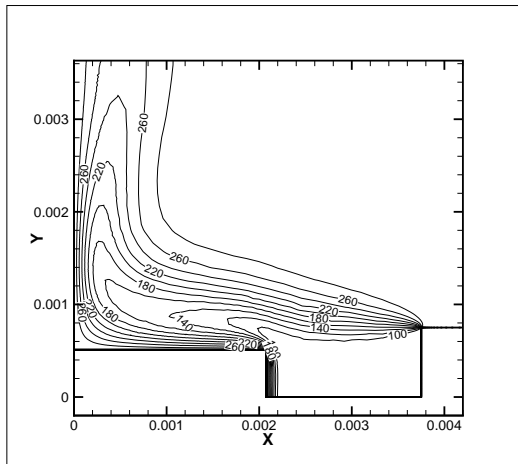
Isothermal plots shown in figures 3.4, 3.5 and 3.6 show the variation of temperature field inside the enclosure for various $\frac{C}{r}$ ratio. The variation of temperature is maximum in the case having low height and width of Fin, with constant $\frac{C}{r}$ ratio and Reynolds number as shown in figure 3.4a, 3.4b, 3.4c and 3.4d. This temperature distribution changes with increasing $\frac{C}{r}$ ratio and almost a constant temperature is observed in the left wall.



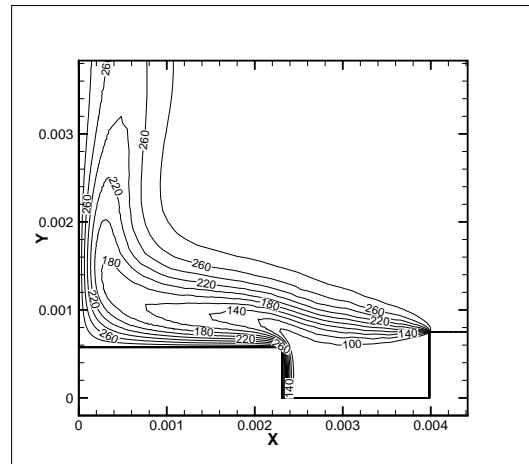
(a) $\frac{C}{r} = 2.23, \frac{H_f}{r} = 1.85$ and $Re = 3708$



(b) $\frac{C}{r} = 2.23, \frac{H_f}{r} = 2.31$ and $Re = 3708$

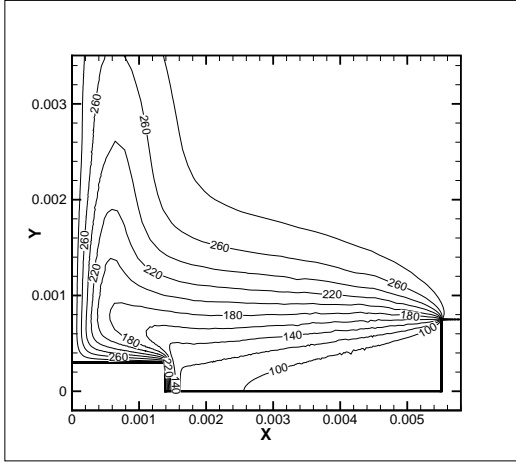


(c) $\frac{C}{r} = 2.23, \frac{H_f}{r} = 2.77$ and $Re = 3708$

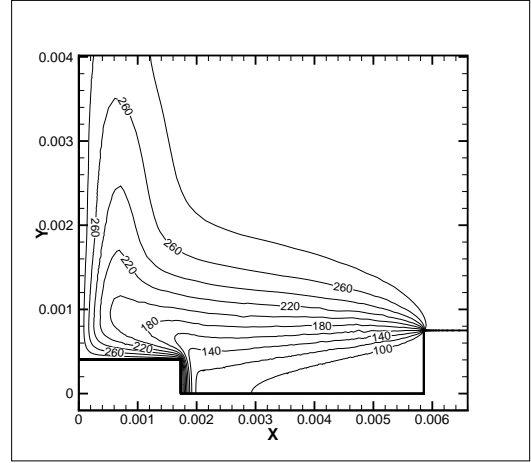


(d) $\frac{C}{r} = 2.23, \frac{H_f}{r} = 3.08$ and $Re = 3708$

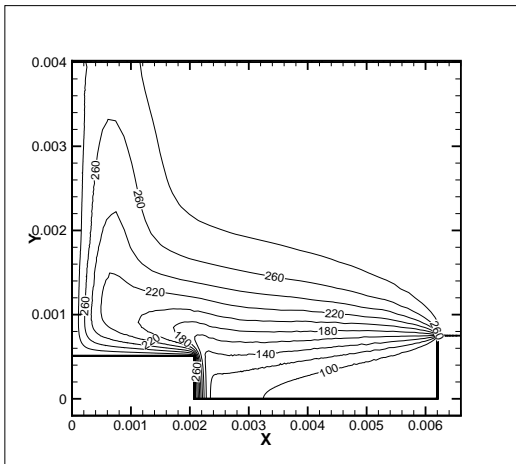
Figure 3.4: isothermal plot for $\frac{C}{r} = 2.23, Re = 3708$



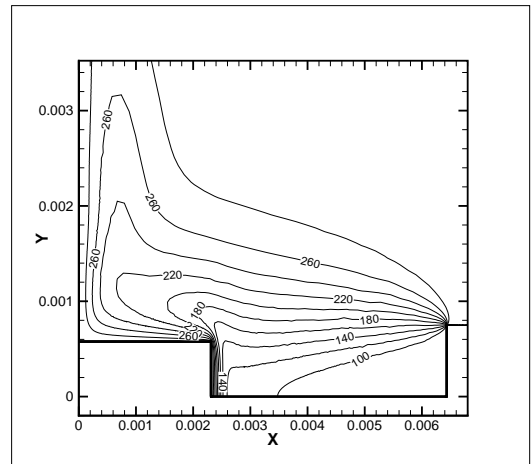
(a) $\frac{C}{r} = 5.5, \frac{H_f}{r} = 1.85$ and $Re = 3708$



(b) $\frac{C}{r} = 5.5, \frac{H_f}{r} = 2.31$ and $Re = 3708$

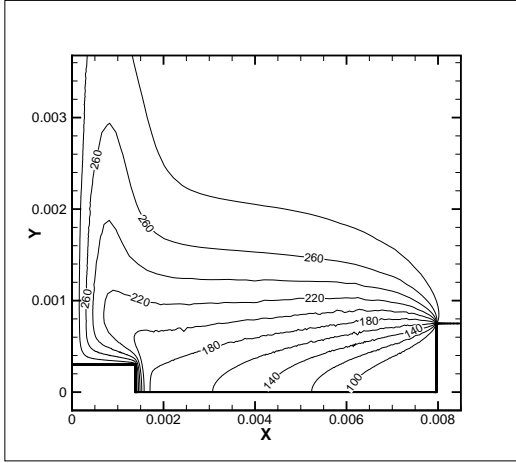


(c) $\frac{C}{r} = 5.5, \frac{H_f}{r} = 2.77$ and $Re = 3708$

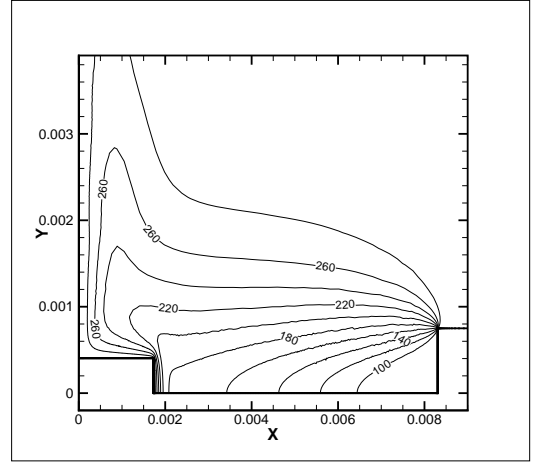


(d) $\frac{C}{r} = 5.55, \frac{H_f}{r} = 3.08$ and $Re = 3708$

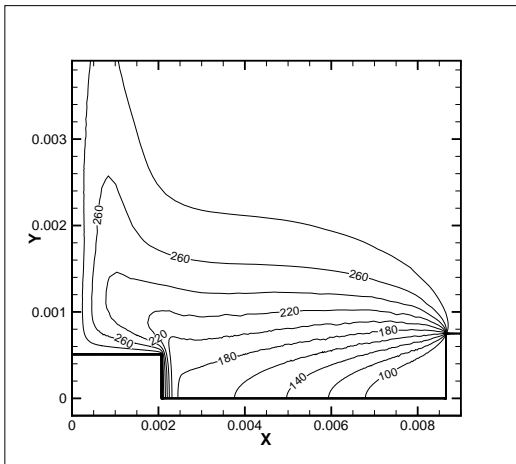
Figure 3.5: isothermal plot for $\frac{C}{r} = 5.5, Re = 3708$



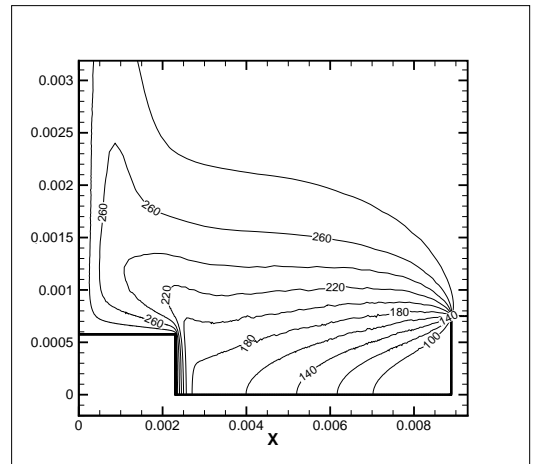
(a) $\frac{C}{r} = 8.77, \frac{H_f}{r} = 1.85$ and $Re = 3708$



(b) $\frac{C}{r} = 8.77, \frac{H_f}{r} = 2.31$ and $Re = 3708$



(c) $\frac{C}{r} = 8.77, \frac{H_f}{r} = 2.77$ and $Re = 3708$



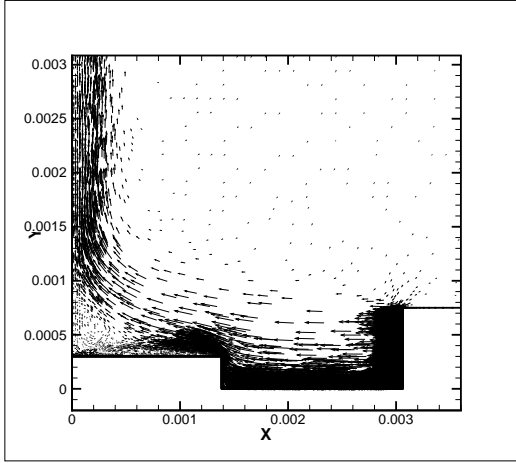
(d) $\frac{C}{r} = 8.77, \frac{H_f}{r} = 3.08$ and $Re = 3708$

Figure 3.6: isothermal plot for $\frac{C}{r} = 8.77, Re = 3708$

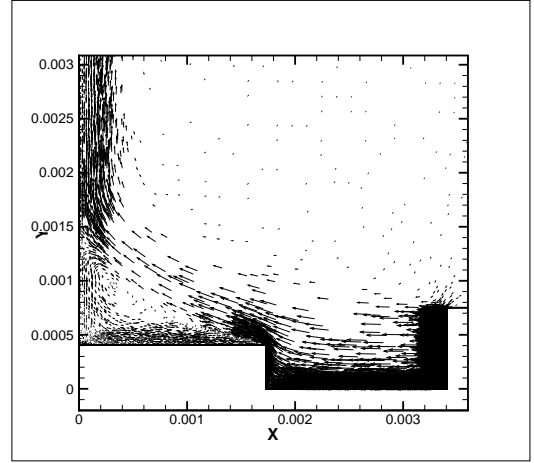
3.2 Heat transfer and fluid flow characteristics of axis symmetry enclosure with Reynolds number 5019

3.2.1 Flow Characteristics

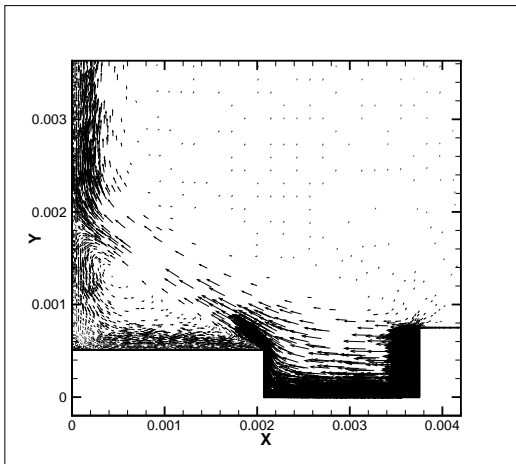
The velocity vector shown in figure 3.7, 3.8 and 3.9 with different jet-to-fin spacing are observed that with change in length and width of fin the bounce off effect area increases. If we compare figure 3.7a, 3.7b and 3.7d we can clearly observed that the bounce back effect increases with increase in width and height of the fin. Also it can be observed that increase in jet-to-fin spacing minimize the velocity due to which for higher jet-to-fin spacing there is no bounce back effect as shown in figure 3.9b, 3.9c and 3.9d.



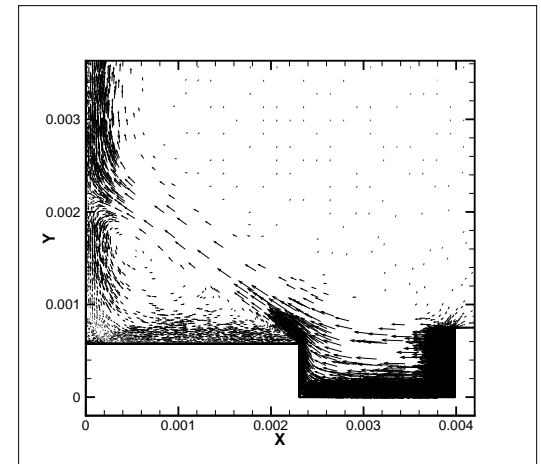
(a) $\frac{C}{r} = 2.23$, $\frac{H_f}{r} = 1.85$ and $Re = 5019$



(b) $\frac{C}{r} = 2.23$, $\frac{H_f}{r} = 2.31$ and $Re = 5019$

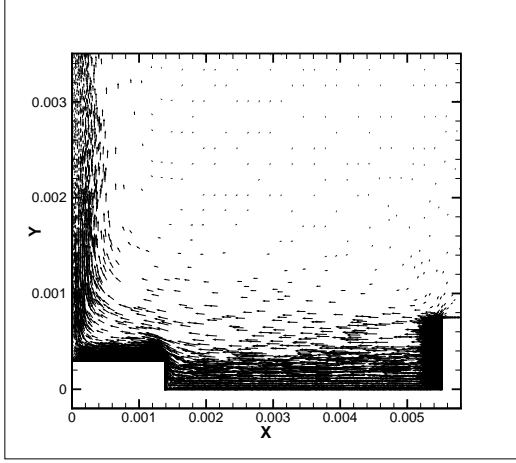


(c) $\frac{C}{r} = 2.23$, $\frac{H_f}{r} = 2.77$ and $Re = 5019$

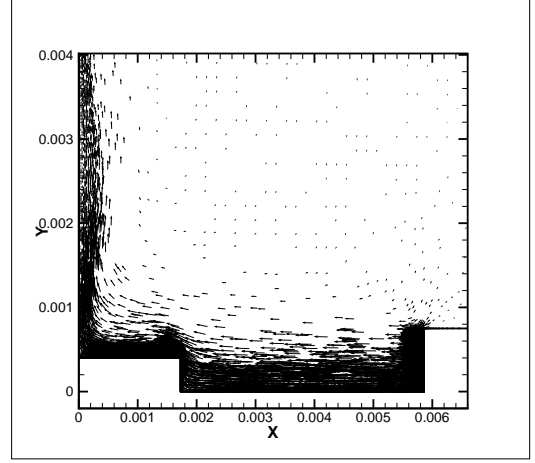


(d) $\frac{C}{r} = 2.23$, $\frac{H_f}{r} = 3.08$ and $Re = 5019$

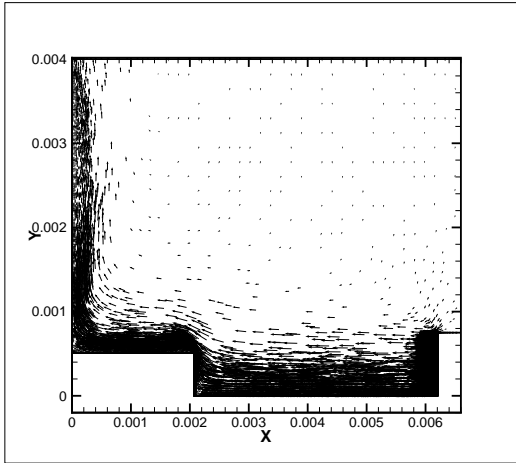
Figure 3.7: vector plots for $\frac{C}{r} = 2.23$, $Re = 5019$



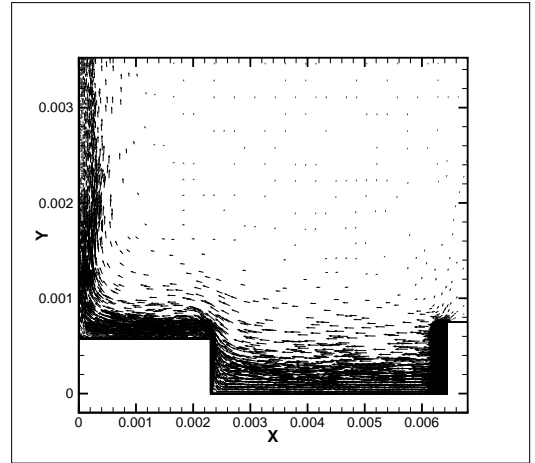
(a) $\frac{C}{r}=5.5$, $\frac{H_f}{r}=1.85$ and $Re=5019$



(b) $\frac{C}{r}=5.5$, $\frac{H_f}{r}=2.31$ and $Re=5019$

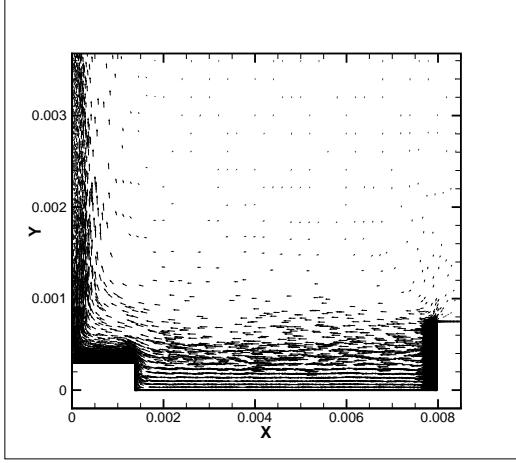


(c) $\frac{C}{r}=5.5$, $\frac{H_f}{r}=2.72$ and $Re=5019$

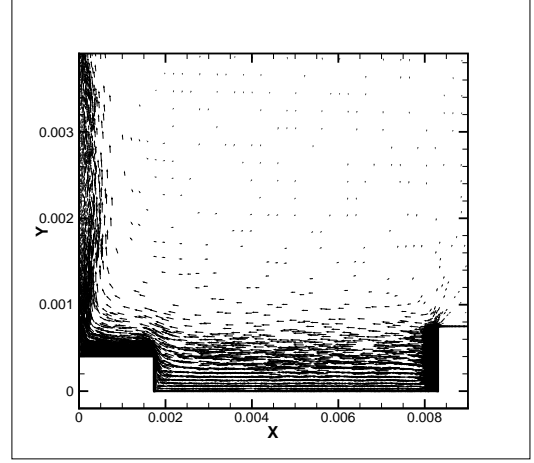


(d) $\frac{C}{r}=5.5$, $\frac{H_f}{r}=3.08$ and $Re=5019$

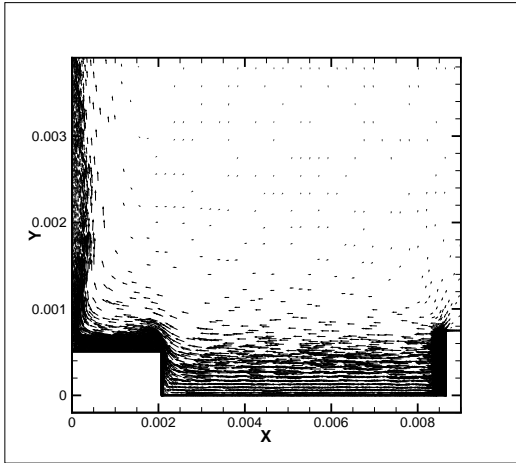
Figure 3.8: Vector plot for $\frac{C}{r}=5.5$, $Re=5019$



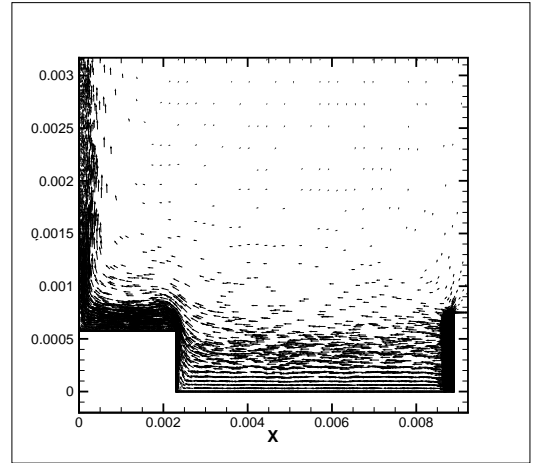
(a) $\frac{C}{r} = 8.77$, $\frac{H_f}{r} = 1.85$ and $Re = 5019$



(b) $\frac{C}{r} = 8.77$, $\frac{H_f}{r} = 2.31$ and $Re = 5019$



(c) $\frac{C}{r} = 8.77$, $\frac{H_f}{r} = 2.77$ and $Re = 5019$

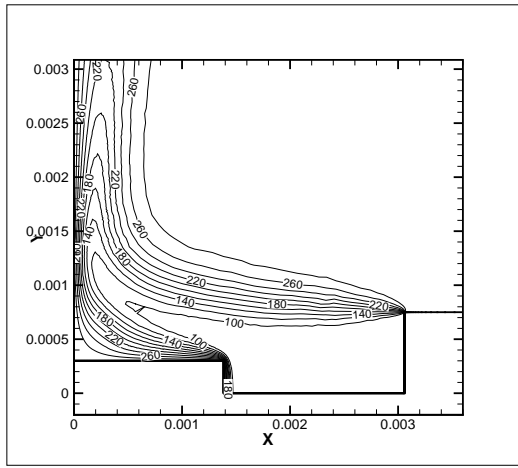


(d) $\frac{C}{r} = 8.77$, $\frac{H_f}{r} = 3.08$ and $Re = 5019$

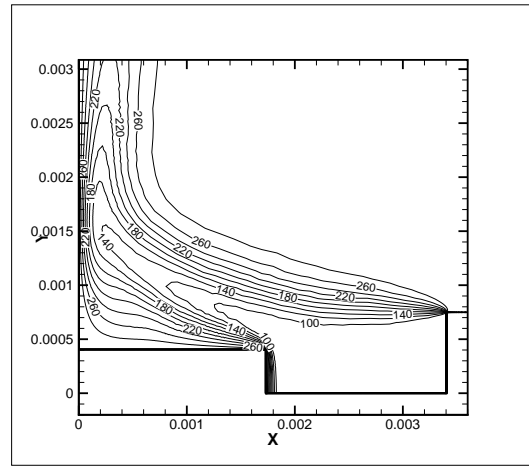
Figure 3.9: Vector plot for $\frac{C}{r} = 8.77$, $Re = 5019$

3.2.2 Heat transfer characteristic

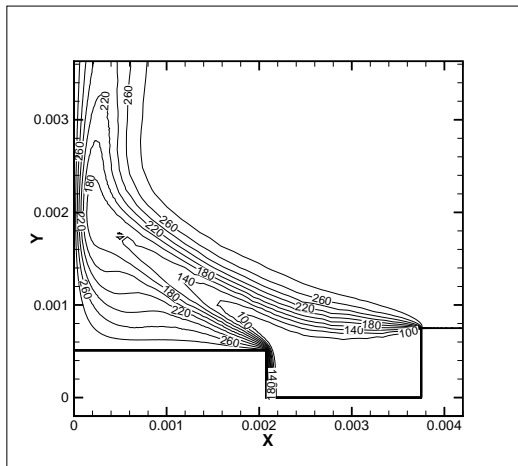
Figures 3.10, 3.11 and 3.12 show the isotherm plot for $Re=5019$. we can observed that for the higher jet-to-fin spacing the temperature variation is less as compared to low jet-to-fin spacing. Here in figure we can observed that for different jet-to-fin spacing with constant width and height of fin the temperature is constant in the wall of fin. The lowest temperature seen is 100 K and 290 K is the highest temperature. For higher jet-to-fin spacing the variation of temperature in flat plate can be seen clearly as compare to low jet-to-fin spacing.



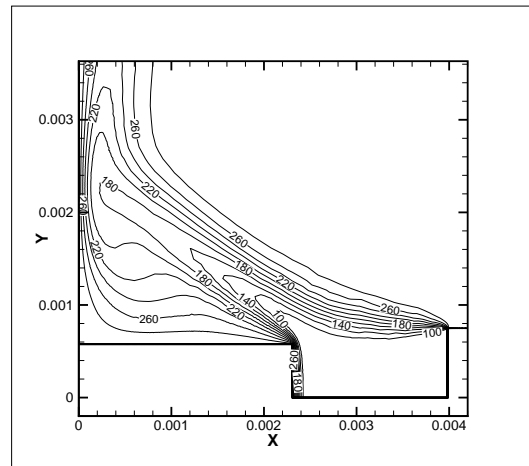
(a) $\frac{C}{r} = 2.23, \frac{H_f}{r} = 1.85$ and $Re = 5019$



(b) $\frac{C}{r} = 2.23, \frac{H_f}{r} = 2.31$ and $Re = 5019$

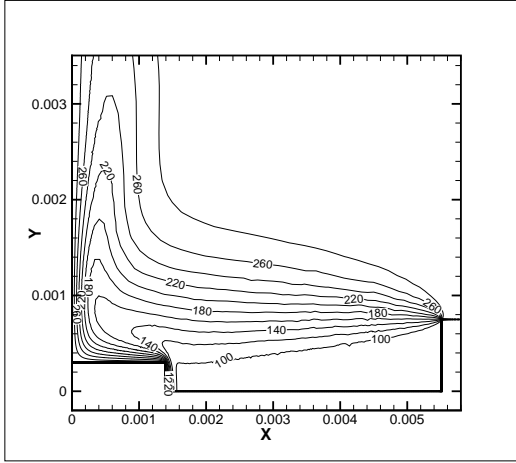


(c) $\frac{C}{r} = 2.23, \frac{H_f}{r} = 2.77$ and $Re = 5109$

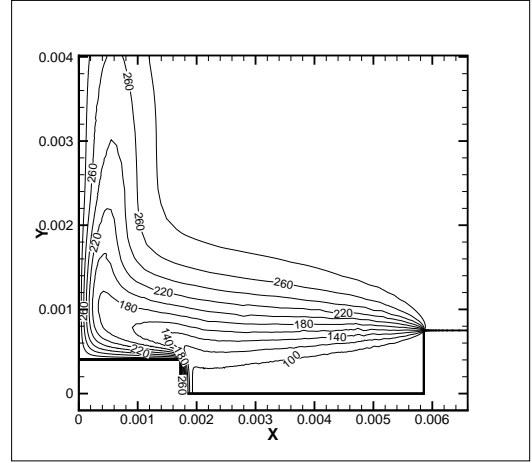


(d) $\frac{C}{r} = 2.23, \frac{H_f}{r} = 3.08$ and $Re = 5109$

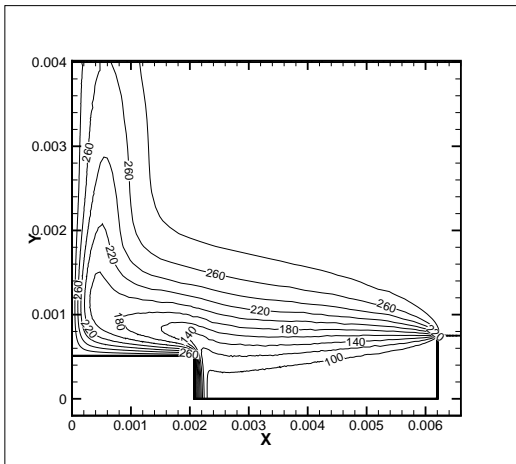
Figure 3.10: isothermal plot for $\frac{C}{r} = 2.23, Re = 5019$



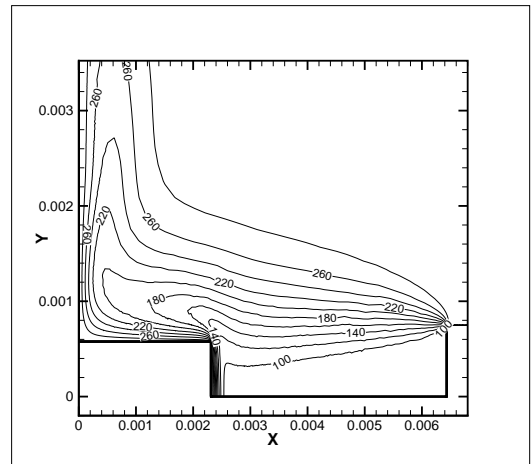
(a) $\frac{C}{r} = 5.5, \frac{H_f}{r} = 1.85$ and $Re = 5019$



(b) $\frac{C}{r} = 5.5, \frac{H_f}{r} = 2.31$ and $Re = 3708$

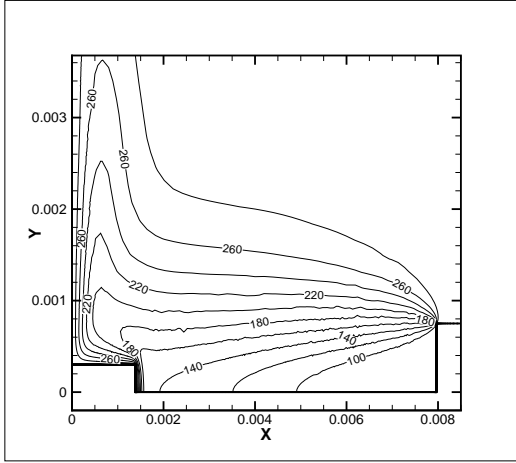


(c) $\frac{C}{r} = 5.5, \frac{H_f}{r} = 2.77$ and $Re = 5019$

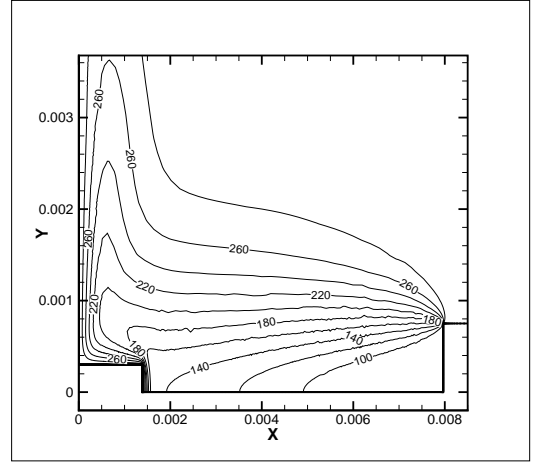


(d) $\frac{C}{r} = 5.55, \frac{H_f}{r} = 3.08$ and $Re = 5019$

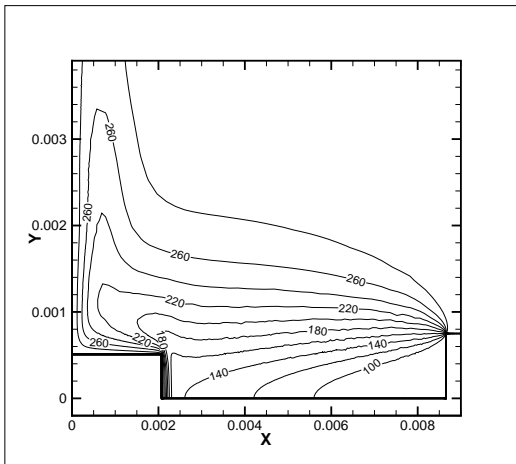
Figure 3.11: isothermal plot for $\frac{C}{r} = 5.5, Re = 5019$



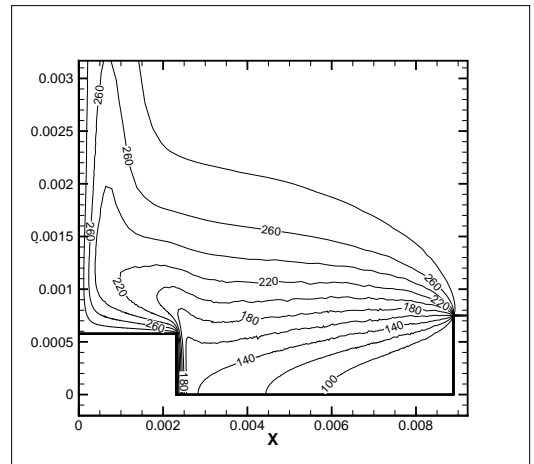
(a) $\frac{C}{r} = 8.77, \frac{H_f}{r} = 1.85$ and $Re = 5019$



(b) $\frac{C}{r} = 8.77, \frac{H_f}{r} = 2.31$ and $Re = 5019$



(c) $\frac{C}{r} = 8.77, \frac{H_f}{r} = 2.77$ and $Re = 5019$



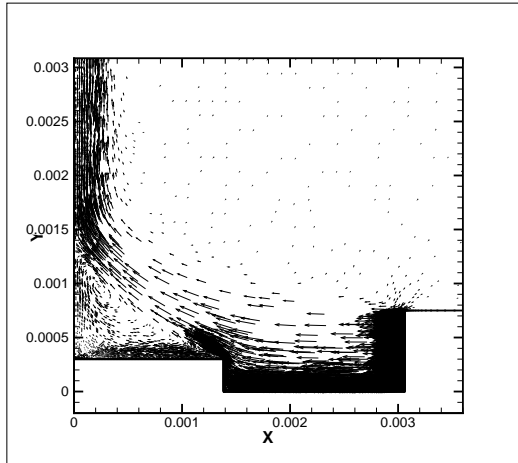
(d) $\frac{C}{r} = 8.77, \frac{H_f}{r} = 3.08$ and $Re = 5019$

Figure 3.12: isothermal plot for $\frac{C}{r} = 8.77, Re = 5019$

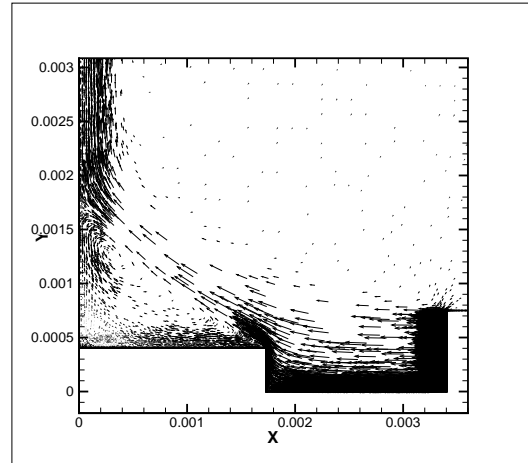
3.3 Heat transfer and fluid flow characteristics of axis symmetry enclosure with Reynolds number 8673

3.3.1 Flow Characteristics

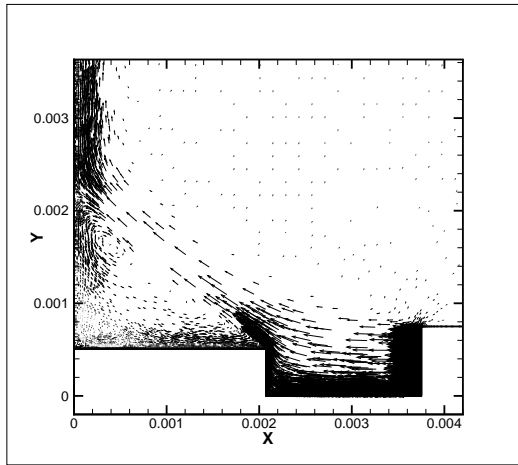
Velocity vector shown in the figure 3.13, 3.14 and 3.15 are the velocity and direction of flow having Reynolds number 8673. Here we can observe that velocity increases with increase in Reynolds number. From figure 3.13a, 3.13b, 3.13c and 3.13d we can clearly see the bounce back effect on the vertical plate, as the width and height of fin increases the lesser the bounce off effect is seen. As compared to figure 3.13a and 3.14a.



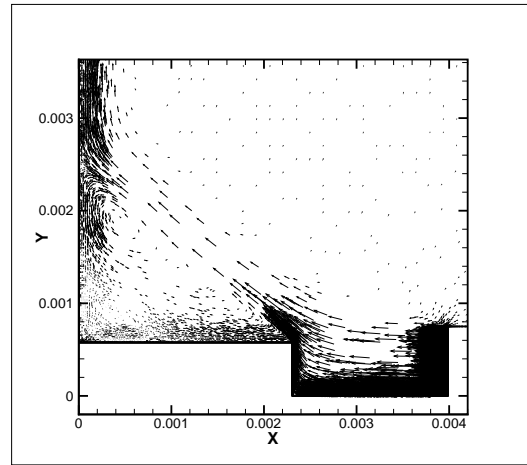
(a) $\frac{C_r}{r} = 2.23$, $\frac{H_f}{r} = 1.85$ and $Re = 8763$



(b) $\frac{C_r}{r} = 2.23$, $\frac{H_f}{r} = 2.31$ and $Re = 8763$

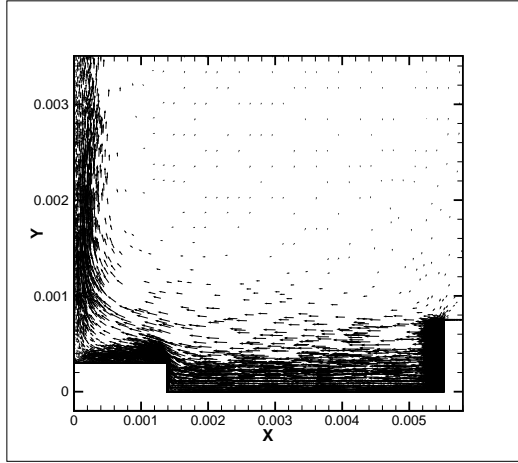


(c) $\frac{C_r}{r} = 2.23$, $\frac{H_f}{r} = 2.77$ and $Re = 8763$

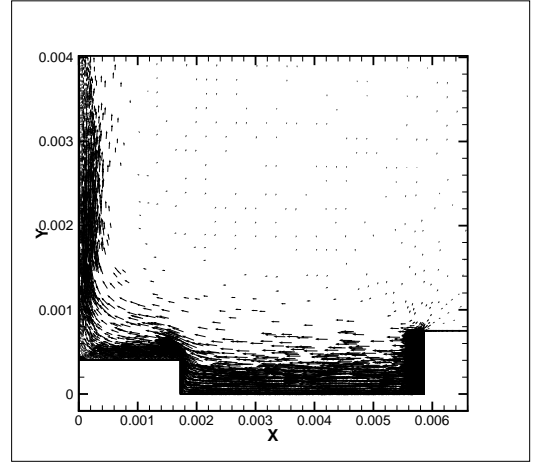


(d) $\frac{C_r}{r} = 2.23$, $\frac{H_f}{r} = 3.08$ and $Re = 8763$

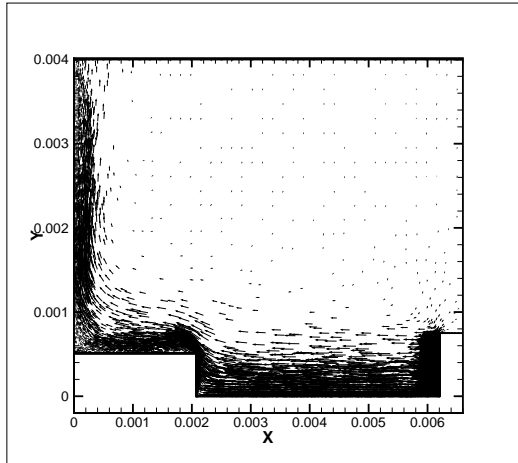
Figure 3.13: vector plots for $\frac{C_r}{r} = 2.23$, $Re = 8763$



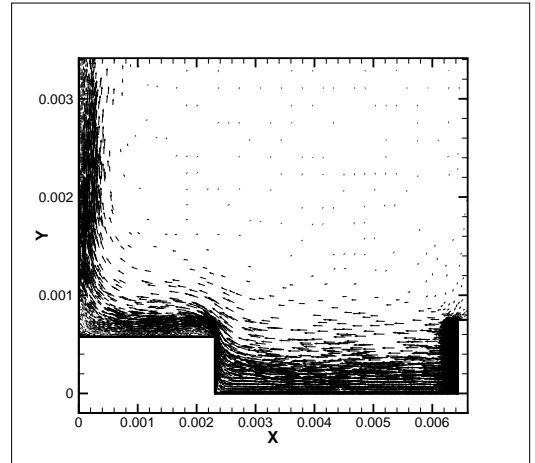
(a) $\frac{C}{r}=5.5$, $\frac{H_f}{r}=1.85$ and $Re=8763$



(b) $\frac{C}{r}=5.5$, $\frac{H_f}{r}=2.31$ and $Re=8763$

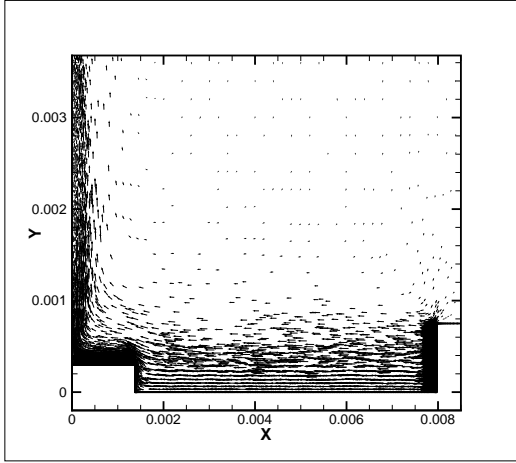


(c) $\frac{C}{r}=5.5$, $\frac{H_f}{r}=2.72$ and $Re=8763$

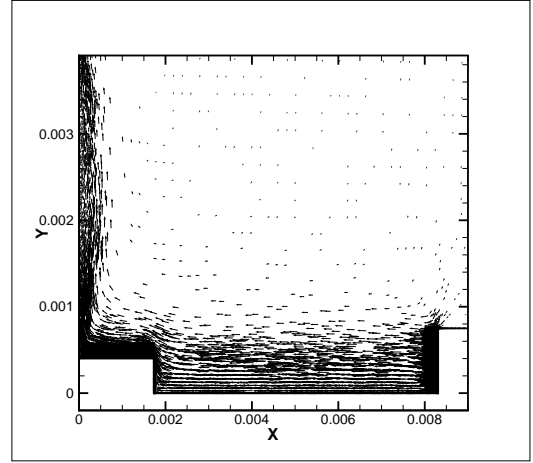


(d) $\frac{C}{r}=5.5$, $\frac{H_f}{r}=3.08$ and $Re=8763$

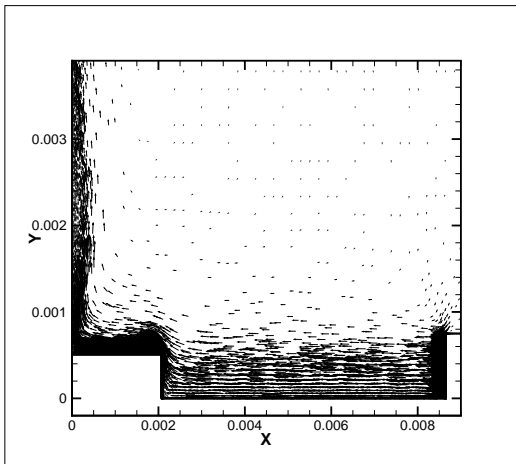
Figure 3.14: Vector plot for $\frac{C}{r}=5.5$, $Re=8763$



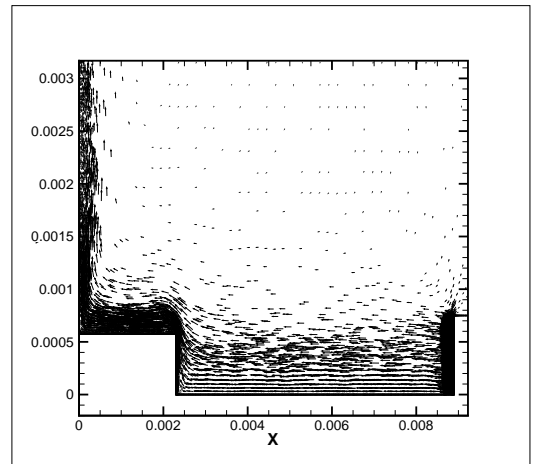
(a) $\frac{C}{r} = 8.77$, $\frac{H_f}{r} = 1.85$ and $Re = 8763$



(b) $\frac{C}{r} = 8.77$, $\frac{H_f}{r} = 2.31$ and $Re = 8763$



(c) $\frac{C}{r} = 8.77$, $\frac{H_f}{r} = 2.77$ and $Re = 8763$

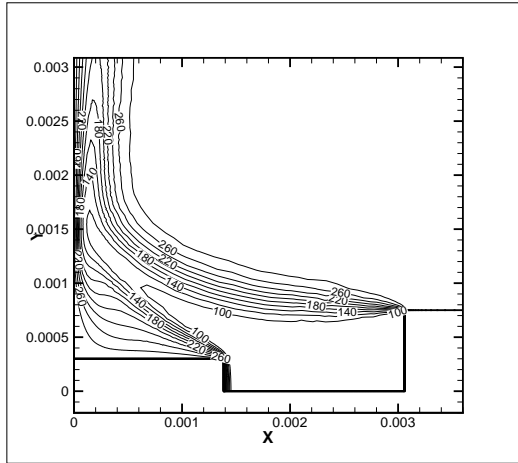


(d) $\frac{C}{r} = 8.77$, $\frac{H_f}{r} = 3.08$ and $Re = 8763$

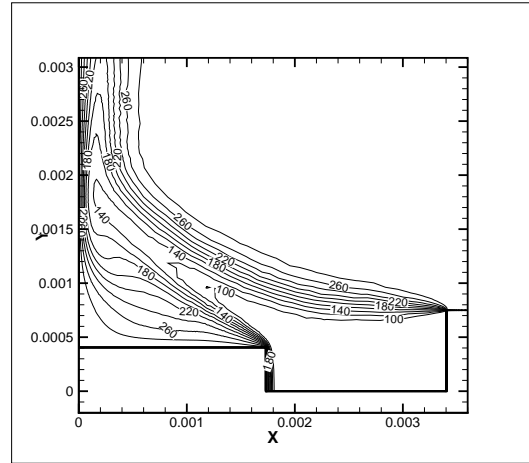
Figure 3.15: Vector plot for $\frac{C}{r} = 8.77$, $Re = 8763$

3.3.2 Heat transfer characteristic

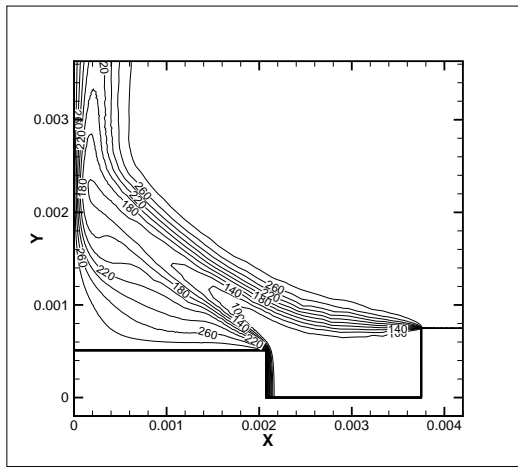
Isothermal plots shown in figures 3.16, 3.17 and 3.18 shows that for lower jet-to-fin spacing the temperature variation is more as compared to high jet-to-fin spacing, therefore the important parameter for better heat transfer is low jet-to-fin spacing.



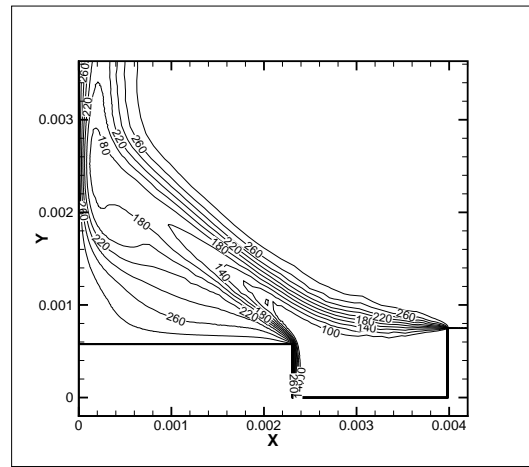
(a) $\frac{C}{r} = 2.23, \frac{H_f}{r} = 1.85$ and $Re = 8763$



(b) $\frac{C}{r} = 2.23, \frac{H_f}{r} = 2.31$ and $Re = 8763$

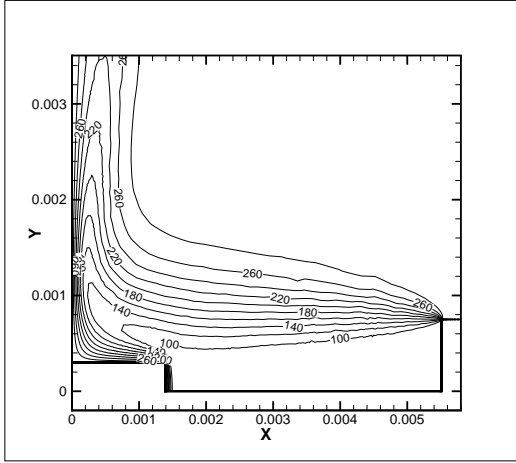


(c) $\frac{C}{r} = 2.23, \frac{H_f}{r} = 2.77$ and $Re = 8763$

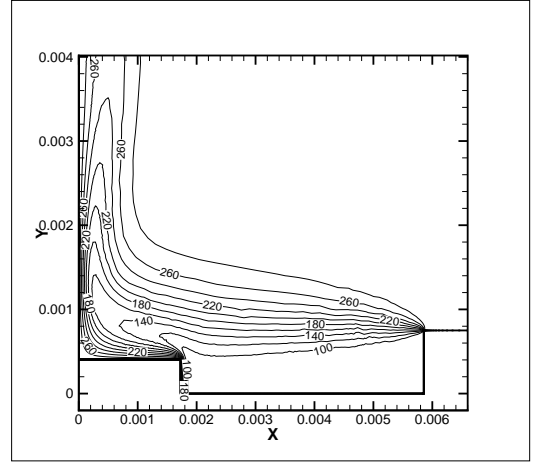


(d) $\frac{C}{r} = 2.23, \frac{H_f}{r} = 3.08$ and $Re = 8763$

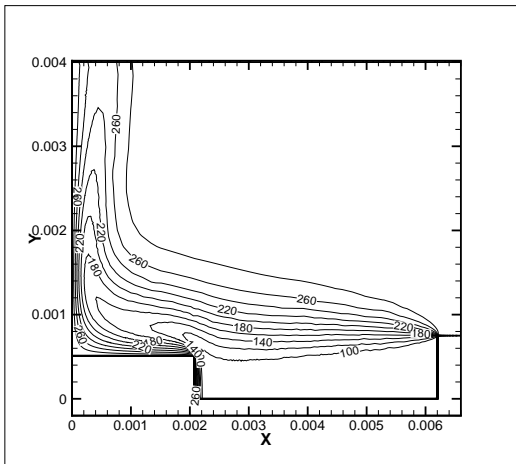
Figure 3.16: isothermal plot for $\frac{C}{r} = 2.23, Re = 8763$



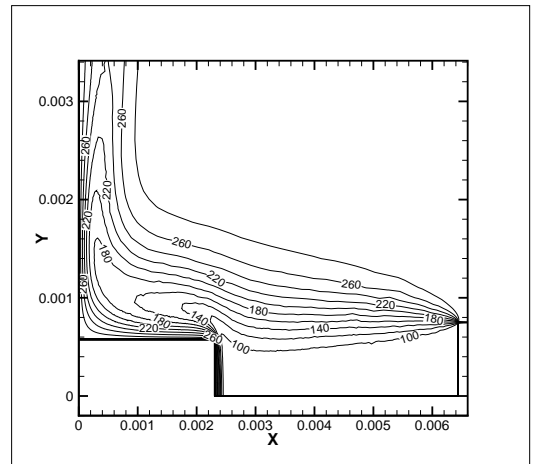
(a) $\frac{C}{r} = 5.5, \frac{H_f}{r} = 1.85$ and $Re = 8763$



(b) $\frac{C}{r} = 5.5, \frac{H_f}{r} = 2.31$ and $Re = 8763$

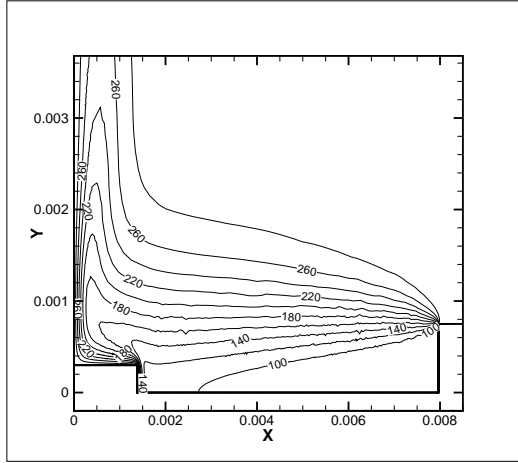


(c) $\frac{C}{r} = 5.5, \frac{H_f}{r} = 2.77$ and $Re = 8763$

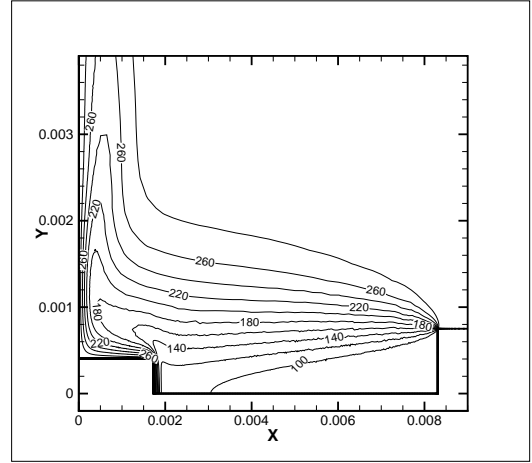


(d) $\frac{C}{r} = 5.55, \frac{H_f}{r} = 3.08$ and $Re = 8763$

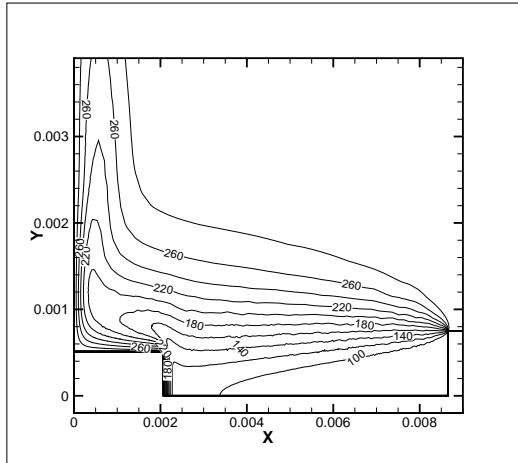
Figure 3.17: isothermal plot for $\frac{C}{r} = 5.5, Re = 8763$



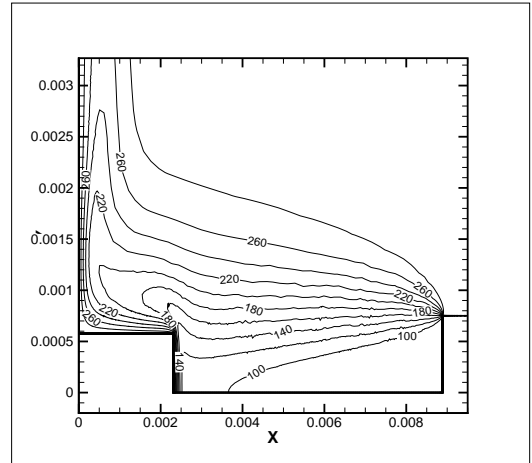
(a) $\frac{C}{r} = 8.77, \frac{H_f}{r} = 1.85$ and $Re = 8763$



(b) $\frac{C}{r} = 8.77, \frac{H_f}{r} = 2.31$ and $Re = 8763$



(c) $\frac{C}{r} = 8.77, \frac{H_f}{r} = 2.77$ and $Re = 8763$



(d) $\frac{C}{r} = 8.77, \frac{H_f}{r} = 3.08$ and $Re = 8763$

Figure 3.18: isothermal plot for $\frac{C}{r} = 8.77, Re = 8763$

3.4 Tabular form of results

The below table 3.2 and figure 3.19 shows the relation between different Reynolds number and $\frac{C}{r}$ ratio With average nusselt number. we can observed that nusselt number increases with increase in Reynolds number. Also we can observed that for each reynolds number there are differen jet-to-fin spacing which shows that average nusselt number not only depends on the Reynolds number but it also depends on jet-to-fin spacing. Here in the table it is clearly seen that if the jet-to-fin spacing is constant and width and height of the fin increases the average nusselt number gradually decreases.

<i>Parameters</i>		\overline{Nu}		
$\frac{C}{r}$	$\frac{H_f}{r}$	<i>Re</i> – 3078	<i>Re</i> – 5019	<i>Re</i> – 8673
2.23	1.85	0.675	0.95	1
2.23	2.31	0.6	0.74	0.8
2.23	2.77	0.5	2.075	2.12
2.23	3.08	0.092	0.121	0.184
5.5	1.85	0.425	0.475	0.77
5.5	2.31	0.587	0.65	1.02
5.5	2.77	1.06	1.27	2.02
5.5	3.08	0.019	0.036	0.094
8.77	1.85	0.325	0.37	0.45
8.77	2.31	0.332	0.38	0.475
8.77	2.77	0.6112	0.75	0.95
8.77	3.08	0.0044	0.0094	0.028

Table 3.2: Average Nusselt number for different $\frac{C}{r}$ ratio

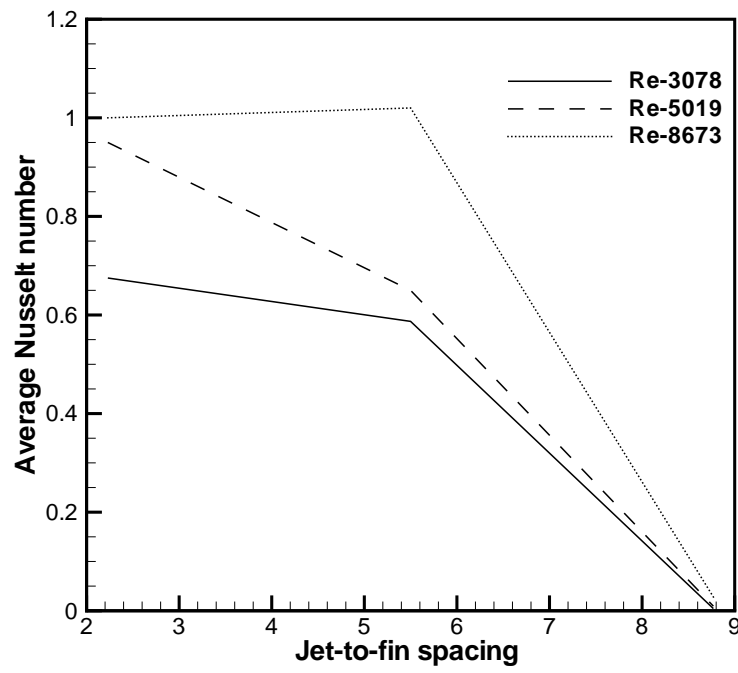


Figure 3.19: Jet-to-nozzle spacing v/s Nusselt number

CHAPTER 4

Conclusion and future work

4.1 CONCLUSION

Numerical simulation are carried out for steady two dimensional laminar natural convection flow of air in a Axis-simmetry domian and the results are discussed in the preceding section. various parameters are studied includes jet-to-fin spacing, width of fin, length of fin and reynolds number to study the behaviors on the temperature and flow field. From the above outlined result following conclusion is drawn:

1. The Jet-to-fin spacing of the domain should not be more, for the better heat transfer..
2. The effect of boundary layer is observed in the high Reynolds number as compared with the low Reynolds number as the driving force increases with the Reynolds number.
3. But as the Reynolds number increases the disturbances could be observed in the enclosure. The perturbations are observed in the vectors plots at corner of the vertical/left wall and fin of the domain suggesting more effective zone to carry any operation there.

4.2 Future works

The current study was generally taken for higher Reynolds number. The simulation can be carried out by using lower Reynolds number and different jet-to-fin spacing.

- The simulation which is carried out can be done experimentally with the data which are obtained from present study.
- The material taken in the simulation can be changed, for current study air is taken as fluid, we can consider liquid nitrogen and liquid helium.

Bibliography

- [1] J. W. Baughn and S. Shimizu. Heat transfer measurements from a surface with uniform heat flux and an impinging jet. *Journal of Heat Transfer*, 111:1096–1098, november 1989.
- [2] Luis A. Brignoni and Suresh V. Garimella. Experimental optimization of confined air jet impingement on a pin fin heat sink. *IEEE*, 22:399–404, 1999.
- [3] Andrew C. Chambers, David R. H. Gillespie, Peter T. Ireland, and Geoffrey M. Dailey. The effect of initial cross flow on the cooling performance of a narrow impingement channel. *Journal of Heat Transfer*, 127:358–365, march 2005.
- [4] Srinath V Ekkad and David Kontrovitz. Jet impingement heat transfer on dimpled target surfaces. *International Journal of Heat and Fluid Flow*, 23:22–28, february 2002.
- [5] Hani A. El-Sheikh and Suresh V. Garimella. Heat transfer from pin-fin heat sinks under multiple impinging jets. *IEEE*, 23:113–120, february 2000.
- [6] Janice A. Fitzgerald and Suresh V. Garimella. A study of the flow field of a confined and submerged impinging jet. *International Journal of Heat and Mass Transfer*, 41:1025–1034, april 1998.

-
- [7] L. W. Florschuetz, R. A. Berry, and D. E. Metzger. Periodic streamwise variations of heat transfer coefficients for inline and staggered arrays of circular jets with cross-flow of spent air. *Journal of Heat Transfer*, 102:132–137, february 1980.
- [8] S. V. Garimella and R. A. Rice. Confined and submerged liquid jet impingement heat transfer. *Journal of Heat Transfer*, 117:871–877, november 1995.
- [9] R.J. Goldstein and W.S. Seol. Heat transfer to a row of impinging circular air jets including the effect of entrainment. *International Journal of Heat and Mass Transfer*, 34:2133–2147, august 1991.
- [10] K. Jambunathan, E. Lai, M.A. Moss, and B.L. Button. A review of heat transfer data for single circular jet impingement. *International Journal of Heat and Fluid Flow*, 13:106–115, june 1992.
- [11] Chin-Yuan Li and Suresh V. Garimella. Prandtl-number effects and generalized correlations for confined and submerged jet impingement. *International Journal of Heat and Mass Transfer*, 44:3471–3480, september 2001.
- [12] Hung-Yi Y. Li, Kuan-Ying Y. Chen, and Ming-Hung H. Chiang. Thermal-fluid characteristics of plate-fin heat sinks cooled by impingement jet. *Energy Conversion and Management*, 50:2748–2746, november 2009.
- [13] J.G. Maveety and H.H. Jung. Heat transfer from square pin-fin heat sinks using air impingement cooling. *IEEE*, 25:459–469, 2002.
- [14] H. Sun, C.F. Ma, and Y.C. Chen. Prandtl number dependence of impingement heat transfer with circular free-surface liquid jets. *International Journal of Heat and Mass Transfer*, 41:1360–1363, may 1998.
- [15] R. Viskanta. Heat transfer to impinging isothermal gas and flame jets. *Experimental Thermal Fluid Science*, 6:111–134, feb 1993.
- [16] Bernhard Weigand and Sebastian Spring. Multiple jet impingement? a review. *Heat Transfer Research*, 42:101–142, 2011.

- [17] Neil Zuckerman and Noam Lior. Impingement heat transfer: Correlations and numerical modeling. *Journal of Heat Transfer*, 127:544–552, may 2005.